Iterative Learning Cascade Control of Continuous Noninvasive Blood Pressure Measurement

Thomas Seel, Thomas Schauer
Control Systems Group
Technische Universität Berlin
Berlin, Germany
seel@control.tu-berlin.de

Sarah Weber, Klaus Affeld
Biofluid Mechanics Lab
Charité - Universitätsmedizin Berlin
Berlin, Germany

***Abstract*—A noninvasive continuous blood pressure measurement technique that has been developed lately requires precise control of the blood flow through a superficial artery. The flow is measured using ultrasound and influenced via manipulating the pressure inside an inflatable air balloon which is placed over the artery. This contribution is concerned with the design and evaluation of a learning cascaded control structure for such measurement devices. Two feedback control loops are designed in discrete time via pole placement and then combined with an iterative learning control. The latter exploits the repetitive nature of the disturbance that is induced by the oscillating arterial pressure. Experimental results indicate that the proposed controller structure yields considerably smaller setpoint deviations than previous approaches.**

***Index Terms*—feedback control, iterative learning control, cascade control, biomedical systems, blood pressure measurement**

I. Introduction

Blood pressure measurement is of vital importance in the diagnosis and treatment of many diseases. In particular, it is the cornerstone for the diagnosis, the treatment and the research on arterial hypertension [17]. For more than one hundred years [9], the sphygmomanometry developed by Riva-Rocci and Korotkoff has been the most common method. Its limitations, however, are becoming increasingly evident and therefore alternative solutions are under investigation [15]. Especially when continuous blood pressure monitoring is desirable, this conventional method is of disadvantage, since it only allows repeated measurements every few minutes. Furthermore, only the maximum and the minimum of the blood pressure curve, i.e. the systolic and the diastolic blood pressure, respectively, are identified. Finally, most devices that use this measurement principle do not meet the standards set by the British Hypertension Society (BHS) protocol and by the US Association for the Advancement of Medical Instrumentation (AAMI) [13].

These problems, and especially the problem of continuous measurement, are overcome by another non-invasive technique that was introduced by Penaz about twenty years ago [16]. The method uses continuous plethysmographic detection of the arterial volume in a given measurement volume and

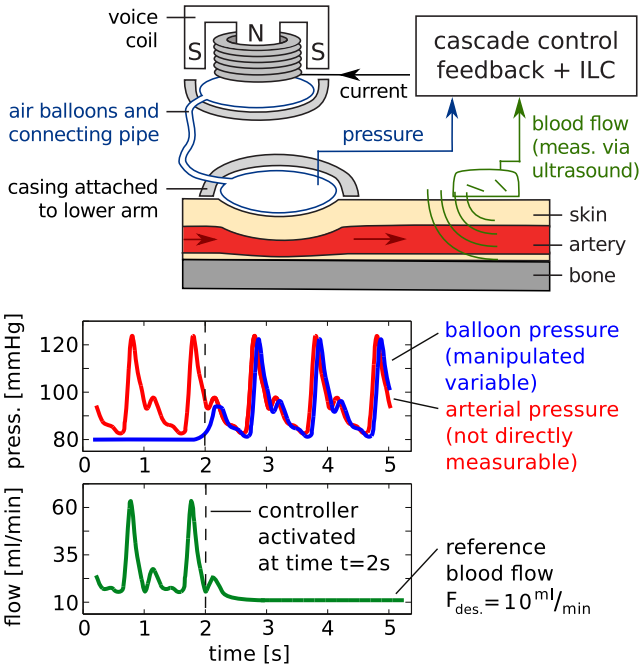

Fig. 1. Non-invasive blood pressure measurement system. A voice coil and two interconnected inflatable air balloons are used to press upon a superficial artery and thus reduce the blood flow, which is measured via a Doppler ultrasound sensor. By controlling this flow to a constant small value, one obtains equality – up to a small constant bias – between the controller-induced balloon pressure and the arterial blood pressure.

closed-loop control for continuously changing the pressure in the measurement volume such that the arterial volume is maintained at a constant value at which the tension of the arterial wall equals zero. Thereby, the desired arterial pressure is obtained as the pressure in the measurement volume. In [23], the original approach is enhanced by using ultrasound to measure the arterial blood flow and maintain it at a small constant value. In that control system, the manipulated variable is the pressure of an inflatable air balloon which is attached to the lower arm such that it pushes upon the radial artery. Again, the periodic pressure curve that is required

978-1-4799-0652-9/13 $31.00 © 2013 IEEE
DOI 10.1109/SMC.2013.378

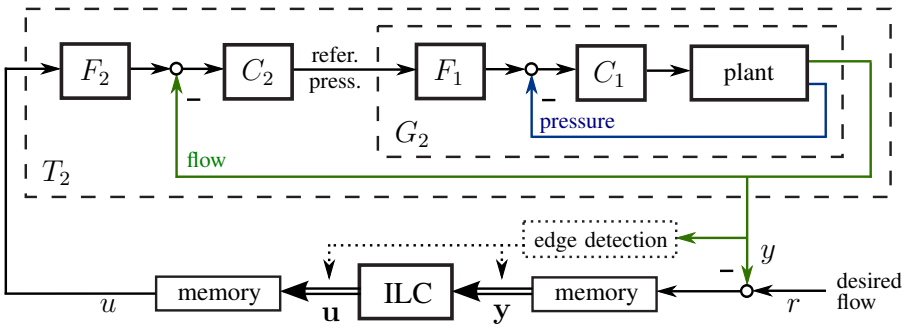

Fig. 2. Block diagram of the controller structure. The plant outputs the pressure, which is controlled by the inner feedback loop, and the flow, which is controlled by the outer feedback loop. Both controllers are two-degree-of-freedom structures consisting of prefilters $F_{1,2}$ and feedbacks $C_{1,2}$. The outermost loop is an iterative learning controller (ILC), which learns in trials triggered by an edge detection of the flow signal. The ILC records the output trajectory of each trial and batch-wise updates the input trajectory that is applied as a reference to the outer feedback control loop.

to achieve this control task equals the desired course of the blood pressure. Figure 1 depicts the main components of the measurement system. In [23], a simple feedback controller was employed to regulate the arterial blood flow. In general, this goal was achieved. However, the ultrasound-based flow measurement is characterized by a bad signal-to-noise ratio. Therefore, setpoint deviations of up to 10 ml/min were obtained.

Regardless of the particular controller, traditional feedback control can only achieve limited bandwidth, and thus limited measurement accuracy, in the presence of measurement noise. In order to improve the controller performance, one may exploit the fact that the blood pressure curve is periodic and exhibits only small changes from one pulse to the next. More precisely, by looking at the pressure and flow curves of subsequent pulses batch-wise we can adapt the balloon pressure curve of the next pulse based on the flow curve of the previous trials and thus introduce a feedback from pulse to pulse. This approach is known as Iterative Learning Control (ILC). See, e.g., [3], [22] for an introduction, and, e.g., [14], [12], [8], [19] for further interest. Applying ILC yields the additional advantage that low-pass filters with zero phase shift can be applied to the noisy flow measurement signal [6]. Therefore, it is expected that controller performance, and thus measurement accuracy, can be improved significantly by the use of ILC.

While ILC has widely been used in robotics and in a a number of process engineering applications (see e.g. [1]), iterative learning control techniques are relatively new to the field of biomedical engineering. However, ILC has been used successfully in blood glucose control [21], in FES-based rehabilitation [7], [20], [18], as well as in robotized surgery, exoskeletons, and rehabilitation robotics [4], [10], [5].

In the present contribution, we examine the challenges and benefits of ILC-methods to the flow control task in the introduced non-invasive continuous blood pressure measurement system. In Section II, a cascaded control structure consisting of two time-discrete feedback controllers surrounded by an Iterative Learning Control is designed. The system identification and model-based controller design is carried out in Section II. Subsequently, the controller performance is evaluated in Section III via repeated experiments with a laboratory model of the cardiovascular system.

II. Controller Design

The experimental setup described in [23] and in Figure 1 is used. Measurable signals include the arterial blood flow via ultrasound and the air balloon pressure. Both signals are obtained at a sample rate of 400 Hz, but the ultrasound signal is low-pass filtered and downsampled to 20 Hz in order to remove some severe noise. The current of the voice coil actuator is set via pulse width modulation at a sample rate of 400 Hz. The larger this current is chosen, the more the actuator pushes on a polyurethane balloon. Via the connecting tube of about 50 cm length, this increase in pressure is forwarded to the pressure balloon over the artery, and thus, the blood flow is reduced. In the following, a control structure is designed to maintain the blood flow at a constantly small value by manipulating the voice coil current. The innermost loop of the cascaded structure is a fast feedback control of the balloon pressure. The reference of this control loop is set by a feedback control of the blood flow. The reference of this loop is updated periodically by an ILC algorithm. A block diagram of this controller structure is given in Figure 1. In the following subsections, the feedback controllers and the ILC are designed. Both for design and verification, a laboratory model of the cardiovascular system is employed. The model can be used to simulate either a constant or a physiologically pulsating arterial pressure. The latter is achieved through an oscillating piston driven by a linear motor. For details, please refer to [23].

A. Pressure and Flow Controller

The design of the pressure controller is a model-based, time-discrete pole placement. In a first step, the dynamics from coil current to balloon pressure are identified by applying a

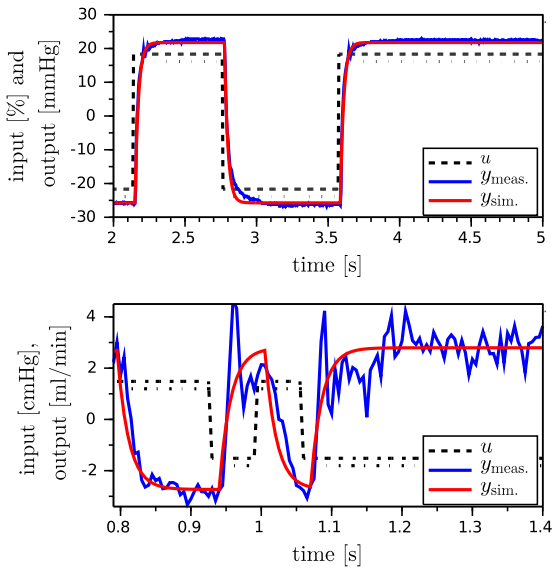

Fig. 3. System identification of the open-loop pressure dynamics and the flow dynamics with closed pressure loop. *Top:* The deviations of the voice coil current and the balloon pressure from their operating point values are plotted as input and output, respectively. *Bottom:* The deviations of the reference pressure and the blood flow from their operating point values are plotted as input and output, respectively. In both cases, a first order transfer function (see (1) and (4)) yields good accordance of simulated and measured data.

pseudo-random binary signal to the current and estimating the parameters of a time-discrete transfer function from the pressure response recorded at 400 Hz. The pressure of the artificial artery is chosen constant during the experiment. Estimation is carried out using standard least-squares techniques, see e.g. [2]. Figure 3 shows that a first-order transfer function with a dead time of three sampling instants is a good approximation of the actual pressure dynamics. More precisely, we obtain:

$$G_1(z) = \frac{22.59z^{-3}}{-0.8098z^{-1}+1}. \tag{1}$$

This result is used to calculate transfer functions of a prefilter $F_1(z)$ and a feedback controller $C_1(z)$ via pole placement. Integral action is included in the feedback controller and the feedback controller is chosen to obtain unity DC-gain. The dominating closed-loop dynamics are chosen to have a rise time of 0.05 s, i.e. twenty samples, and a damping of 0.9. The resulting controller transfer functions are

$$F_1(z) = \frac{0.6831z}{-2.5384+3.2215z}, \tag{2}$$

$$C_1(z) = \frac{-0.0085z^2+0.011z^3}{-0.236+0.0081z-0.7721z^2+z^3}. \tag{3}$$

In a similar manner, the flow controller is designed. A pseudo-random binary signal is applied to the reference of the pressure control loop and the response of the ultrasound blood flow signal is recorded at 20 Hz. Least-squares parameter estimation yields the following first-order transfer function with a dead

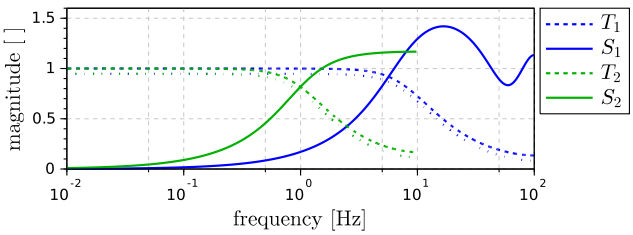

Fig. 4. Sensitivity plots of the closed-loop transfer functions of the inner and outer feedback control loop. Dashed lines indicate the gain of the (noise attenuation- and reference tracking-related) complementary sensitivity functions, while the continuous lines represent the gain of the (disturbance rejection-related) sensitivity functions. Both controllers are designed to yield a damping of 0.9, but the inner loop exhibits a significantly larger bandwidth.

time of three sampling instant:

$$G_2(z) = \frac{-0.0488z^{-3}}{-0.7353z^{-1}+1}. \tag{4}$$

Figure 3 shows that this approximates the actual flow dynamics well. The prefilter $F_2(z)$ and a feedback controller $C_2(z)$ are designed to yield a rise time of 0.6 s, i.e. twelve samples, and a damping of 1 via pole placement. As before, integral action is used in the feedback controller while unity gain of the closed-loop system is assured by the prefilter. This results in the following transfer functions:

$$F_2(z) = \frac{-0.1391z}{0.3527-0.4918z}, \tag{5}$$

$$C_2(z) = \frac{2.1161z^2-2.9506z^3}{-0.1403+0.0048z-0.8645z^2+z^3}. \tag{6}$$

Figure 4 provides sensitivity plots of both control loops. The inner loop is significantly faster than the outer loop. Although the ultrasound signal has been low-pass filtered, it still contains a high level of noise with frequencies from 5 Hz to 10 Hz, as can be seen in Figure 3. Therefore, the rise time of the flow control can hardly be decreased without amplifying this noise. As a result, this standard feedback control is not fast enough to maintain the flow at a constant value when the laboratory model is switched to provide a physiologically pulsating arterial pressure. Only the largest peaks in the flow signal are attenuated. This has been observed before in [23] and is also demonstrated by the flow profile of the first iteration in Figure 7.

B. Iterative Learning Control

As a result of the previous section, we obtained a damped, but still oscillating flow signal when running the artery model with physiologically pulsating blood pressure. In order to eliminate these repeating deviations from the reference value, an Iterative Learning Controller is designed. However, continuous reduction of the blood flow through the artery is not desired from a medical point of view. Therefore, we control the blood flow only in every fourth and fifth pulse, i.e. we alternate between letting three pulses pass and activating the controller for approximately two pulses, as depicted in Figure 5. The double pulses in which the controllers are

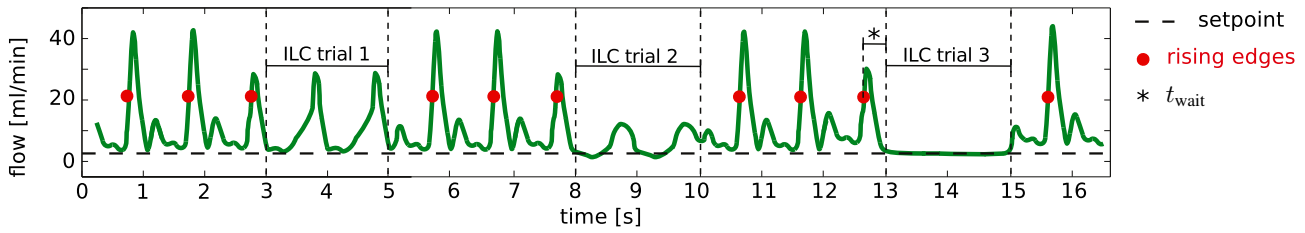

Fig. 5. Synchronization of the ILC trials with the pulses of the artificial cardiovascular system via edge detection. After the third rising edge of the flow signal, the two feedback control loops are closed. The ILC is activated after another time period t_{wait} has passed, where t_{wait} is chosen such that the feedback controllers are given enough time to converge, and such that each ILC trial starts at the end of a falling edge. All controllers are deactivated at the end of each trial, and the edge detection starts to count from zero.

active are defined as the trials (or passes) of the ILC. In each of these trials, a feedforward control input will be applied which is updated between the trials based on measurement information from previous trials.

The ILC is designed in the lifted framework of repetitive discrete-time systems, see e.g. [3]. At a pulse rate f_p and a sample rate of $f_s = 20\,\text{Hz}$, the trial duration (or pass length) is $n = \lceil 2f_s/f_p \rceil$ samples. In every trial $j \in \mathbb{N}^+$, the n sample values of the measured blood flow $y(t)$ are recorded and stacked in the following lifted vector

$$\mathbf{y}_j = [y_j(1/f_s), ..., y_j(n/f_s)]^T, \quad \mathbf{y}_j \in \mathbb{R}^n. \tag{7}$$

The manipulated variable of the ILC shall be denoted $u(t)$ and is added to the reference of the feedback flow controller (see Figure 2). The n samples of that output which are modified by the ILC algorithm are stacked in the lifted vector

$$\mathbf{u}_j = [u_j(1/f_s - d), ..., u_j(n/f_s - d)]^T, \quad \mathbf{u}_j \in \mathbb{R}^n, \tag{8}$$

where d is a controller parameter that is chosen to eliminate dead time and delay in the system dynamics. Furthermore, a constant flow reference value with lifted vector $\mathbf{r} \in \mathbb{R}^n$ is defined. During the first trial, the input is chosen constant at $\mathbf{u_1} = \mathbf{r}$. At the end of each trial, the recorded deviation $\mathbf{e}_j$ between the flow $\mathbf{y}_j$ and its reference value $\mathbf{r}$ is used to update the input $\mathbf{u}$ via the following learning law

$$\mathbf{u}_1 = \mathbf{r}, \quad \mathbf{u}_{j+1} = \mathbf{Q}(\mathbf{u}_j + \lambda(\mathbf{r} - \mathbf{y}_j)), \quad j = 1, 2, \dots, \tag{9}$$

where λ is the learning gain, and $\mathbf{Q}$ is the lifted system matrix of a non-causal low-pass filter. More precisely, $\mathbf{Q}$ is a symmetric Toeplitz matrix containing the Markov parameters of a second-order Butterworth filter, whose cutoff frequency $f_\mathbf{Q}$ serves as a tunable controller parameter. It is introduced because it increases robustness, though at the cost of a non-zero steady state error, see e.g. [3]. The learning gain λ is a positive scalar that can be increased to obtain faster convergence while getting closer to overshooting, and thus to instability. In order to assess stability in the iteration domain formally, a model of the plant is required. From (4), (5), and (6) we calculate the following closed-loop transfer function of the feedback controlled system (cf. Figure 2):

$$T_2(z) = \frac{F_2(z)\,C_2(z)\,G_2(z)}{1 + C_2(z)\,G_2(z)} = \frac{0.0407}{0.6405z - 1.5998z^2 + z^3} \tag{10}$$

By calculating the first n Markov parameters p_i of $T_2(z)$, we obtain the following lifted system matrix:

$$\mathbf{P} = \begin{pmatrix} p_1 & 0 & \cdots & 0 \\ p_2 & p_1 & \cdots & 0 \\ \vdots & \vdots & \ddots & \vdots \\ p_n & p_{n-1} & \cdots & p_1 \end{pmatrix}, \quad \begin{matrix} p_1 = 0.0407 \\ p_2 = 0.0651 \\ p_3 = 0.0781 \\ \vdots \end{matrix} \tag{11}$$

It is a standard result from the ILC literature (see e.g. [3], [12]), that stability in the iteration domain can be assessed via the following criterion:

$$\lim_{j\to\infty} \mathbf{e}_j =: \mathbf{e}_\infty \,\forall \mathbf{u}_0 \;\Leftrightarrow\; \rho(\mathbf{Q}(\mathbf{I} - \lambda\mathbf{P})) < 1 \tag{12}$$

$$\mathbf{e}_\infty = 0\,\forall \mathbf{r} \;\Leftrightarrow\; \mathbf{Q} = \mathbf{I} \tag{13}$$

where ρ denotes the spectral radius. Similarly, monotonic convergence of the Euclidean norm of the error can be assessed via the criterion (see e.g. [3])

$$\bar{\sigma}(\mathbf{PQP^{-1}}(\mathbf{I} - \mathbf{LP})) \leq 1 \;\Rightarrow\; ||\mathbf{e}_{j+1} - \mathbf{e}_\infty||_2 \leq ||\mathbf{e}_j - \mathbf{e}_\infty||_2 \,\forall j\,, \tag{14}$$

where $\bar{\sigma}$ denotes the maximum singular value, i.e. the induced matrix norm of the Euclidean vector norm. In order to pre-estimate suitable ILC parameters, we calculate $\rho(\mathbf{Q}(\mathbf{I} - \lambda\mathbf{P}))$ and $\bar{\sigma}(\mathbf{PQP^{-1}}(\mathbf{I} - \mathbf{LP}))$ for a large number of learning gains λ and Q-filter cutoff frequencies, see Figure 6. It is found that the fastest convergence should be expected for a large $f_\mathbf{Q}$ at about 1 Hz and a learning gain of $\lambda \approx 1.5$, while values below $\lambda \approx 1$ and above $\lambda \approx 3$ are likely to cause transient growth. However, both of the above criteria are conservative in some sense, and they do not make statements on the magnitude of the steady-state error. Hence the results from Figure 6 will only serve as a starting point for the experimental analysis in Section III.

Before, however, we shall shortly comment on the issue of repeatability in this non-standard ILC application. Even with the most elaborate design, the ILC can only eliminate repeating deviations. However, if the blood pressure profile

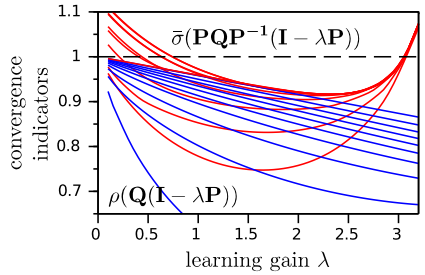

Fig. 6. Spectral radius (blue) and maximum singular value (red) of the lifted closed-loop dynamics matrix over learning gain. Both lines are plotted for a set of Q-filter cutoff-frequencies ranging from the Nyquist frequency of 10 Hz (uppermost curves) down to $f_{\mathbf{Q}} = 1$ Hz (lowest curves). As indicated by the dashed line, asymptotic stability and monotonic convergence can be achieved for $\lambda < 3$, while decreasing $f_{\mathbf{Q}}$ seems to improve the rate of convergence.

does not change too much from one activation phase to the next, then the ILC faces roughly the same control task with the same disturbances in each trial. Furthermore, it needs to be ensured that the activation is synchronized properly with the pulses. Figure 5 illustrates the strategy that is used for synchronization of the ILC with the pulses. While the controllers are inactive, the rising edges in the flow signal are detected. As soon as three edges have been detected, both feedback controllers are activated and the edge detection is turned off. The ILC, however, waits another adjustable time period t_{wait} and then starts to apply the n samples of the stored input trajectory. This strategy ensures that the ILC is always activated at the same instant of a pulse, i.e. shortly before the minimum of the flow signal. Another d sample instants later, the recording of the output trajectory is started. After the n^{th} sample has been recorded, all controllers are turned off, and the edge detection is reactivated.

III. Experimental Results

The artery model is set to provide a physiologically pulsating blood pressure, and the three control loops are activated subsequently. More precisely, we choose a pulse rate of $f_p = 1$ Hz, which results in a pass length of $n = 35$. While the parameters of the classic feedback pressure and flow controller remain constant, we evaluate the learning behavior for various Q-filter cutoff frequencies $f_{\mathbf{Q}}$ and learning gains λ in a sequence of experiments. The experiments differ slightly in positioning of the ultrasound sensor, in the value of the flow reference, ranging from 4 ml/min to 10 ml/min, and in the concentration of the tracer particles of the liquid running through the artificial artery. In accordance with the theoretic predictions of Section II-B, small values for $f_{\mathbf{Q}}$ and λ are found to yield slow convergence and some significant steady-state errors. For larger cutoff frequencies and learning gains, the convergence rate is increased, but for values above $\lambda \approx 2$ divergence and overshooting is observed in some experiments. Figure 7 shows the results of an experiment with rather fast convergence. Therein, the Q-filter is not

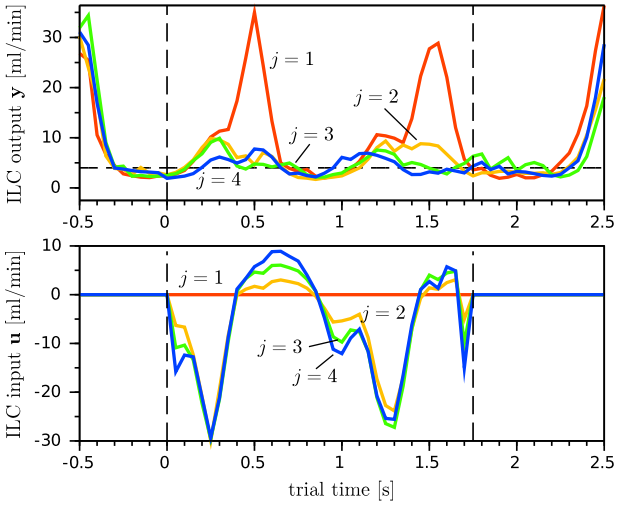

Fig. 7. Iterative Learning Control ($d = 5$, $f_{\mathbf{Q}} = 10$ Hz, $\lambda = 1$) of the blood flow through an artificial artery. *Top:* Within one step of learning the flow is reduced to the constantly small reference value of 4 ml/min indicated by the horizontal dashed line. Vertical dashed lines indicate the beginning and end of the ILC trials. *Bottom:* The input of the ILC, which is fed as a reference to the flow feedback loop, is adjusted from trial to trial based on the measured error and the ILC update law (9). Compared to the first update, changes from the second to the fourth iteration are only minor.

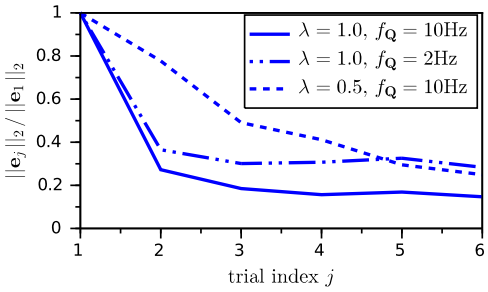

Fig. 8. Convergence of the error for different ILC parameters. For $\lambda = 0.5$, convergence is slow. When using a Q-filter with $f_{\mathbf{Q}} = 2$ Hz, the steady-state error is unacceptably large. However, for $\lambda = 0.5$ and $\mathbf{Q} = \mathbf{I}$, the Euclidean norm of the error is quickly reduced to about 15% of its initial value and remains at this level in the following trials.

active, i.e. $\mathbf{Q} = \mathbf{I}$. However, only the repeating components of the setpoint deviation are eliminated. Iteration-variant disturbances and noise lead to an almost constant root mean square error (RMSE) of 1.7 ml/min.

IV. Conclusion

Control of the arterial blood flow via a voice coil actuator and two air balloons for pressure transmission was considered. We proposed a cascaded controller structure consisting of two time-discrete feedback controllers with prefilters and an iterative learning control. Controller design was based on linear plant models identified from experimental data. The performance of the resulting controller was evaluated

in a number of experiments using a laboratory model of the cardiovascular system including an artificial artery and a physiologically pulsating blood pressure. Results show that, unlike classic feedback control, ILC is able to control the blood flow to a constantly low value at a small root mean square error of below 2 ml/min. However, parameter variations and measurement noise limit the possibilities to reach even smaller setpoint deviations.

One major drawback of the current ILC implementation and most of the available ILC methods is that they cannot handle the case of variable heart rate. The reason is that, in classic ILC theory, the pass length is assumed to be the same for each trial. Therefore, our future work will address this issue and will, on the one hand, include the development of a suitable controller for variable heart rates. On the other hand, we will focus on useful extensions of ILC methods, such as in [11] and [19]. Beyond this, it seems promising to further improve the quality, especially the signal-to-noise ratio, of the Doppler ultrasound flow measurement in order to improve controller performance.

ACKNOWLEDGMENT

The authors would like to thank Florian Heptner and Ralph Stephan for their dedication to the project and in particular for programming the microcontroller for data acquisition and hardware control as well as the PC interface. Furthermore, we highly acknowledge Peter Scharfschwerdt's support with the electronics and with the experiments.

REFERENCES

[1] H.S. Ahn, Y.Q. Chen, and K.L. Moore. Iterative learning control: brief survey and categorization 1998-2004. *IEEE Transactions on SMC, Part C: Applications and Reviews*, 37(6):1099–1121, 2007.

[2] K.J. Astrom, B. Wittenmark. Computer Controlled Systems – Theory and Design. 1984.

[3] D.A. Bristow, M. Tharayil, A.G. Alleyne. A Survey of Iterative Learning Control. *IEEE Control Systems Magazine*, 26(3):69–114, 2006.

[4] B. Cagneau, N. Zemiti, D. Bellot, G. Morel. Physiological motion compensation in robotized surgery using force feedback control. *2007 IEEE International Conference on Robotics and Automation*, 1881-1886, 2007.

[5] A. Duschau-Wicke, A. Morger, H. Vallery, R. Riener. Adaptive Patient Support for Rehabilitation Robots. *at - Automatisierungstechnik*, 58(5):260-268, 2010.

[6] H. Elci, R.W. Longman, M.Q. Phan, J.N. Juang, and R. Ugoletti. Simple Learning Control Made Practical by Zero-Phase Filtering: Applications to Robotics. *IEEE Transactions on Circuits and Systems I: Fundamental Theory and Applications*, 49(6):753–767, 2002.

[7] C.T. Freeman, A.-M. Hughes, J.H. Burridge, P.H. Chappell, P.L. Lewin, E. Rogers. Iterative learning control of FES applied to the upper extremity for rehabilitation. *Control Engineering Practice*, 17(3):368-381, 2009.

[8] K. Galkowski, J. Lam, E. Rogers, S. Xu, B. Sulikowski, W. Paszke and D.H. Owens. LMI based stability analysis and robust controller design for discrete linear repetitive processes. *International Journal of Robust and Nonlinear Control*, 13:1195–1211, 2003.

[9] W. Lewis. The evolution of clinical sphygmomanometry. *Bulletin of the New York Academy of Medicine*, 17(11):871881, 1941

[10] J. Liu, Y. Wang, H. Tong, R.P.S. Han. Iterative Learning Control Based on Radial Basis Function Network for Exoskeleton Arm. *Advanced Materials Research*, Vols.415-417:116-22, 2012.

[11] K.L. Moore, M. Ghosh, Y.Q. Chen. Spatial-based iterative learning control for motion control applications. *Meccanica*, 42(2):167-175, 2007.

[12] M. Norrlöf and S. Gunnarsson. Time and frequency domain convergence properties in iterative learning control. *International Journal of Control*, 75(14):1114–1126, 2002.

[13] E. OBrien. Blood pressure measuring devices: recommendations of the European Society of Hypertension. *British Medical Journal*, 322(7285):531-536, 2001.

[14] D.H. Owens and J. Hätönen. Iterative learning control - An optimization paradigm. *Annual Reviews in Control*, 29:57–70, 2005.

[15] G.Parati, G. Bilo, G. Mancia. Blood pressure measurement in research and in clinical practice: recent evidence. *Current Opinion in Nephrology and Hypertension*, 13(3):343-357, 2004.

[16] J. Penaz. Method and apparatus for automatic non-invasive blood pressure measurement. European Patent No. EP 0284095, 1993.

[17] F. Rabbia, S. Del Colle, E. Testa, D. Naso, F. Veglio. Accuracy of the blood pressure measurement. *Minerva cardioangiologica*, 54(4):399-416, 2006.

[18] T. Seel, M. Valtin, T. Schauer. Design and Control of an Adaptive Peroneal Stimulator with Inertial Sensor-based Gait Phase Detection. *18th International FES Society Conference*, 2013.

[19] T. Seel, T. Schauer, J. Raisch. Iterative Learning Control for Variable Pass Length Systems. *Proc. of the IFAC World Congress*, pp. 4880-4885, 2011. http://dx.doi.org/10.3182/20110828-6-IT-1002.02180

[20] A. Soska, C.T. Freeman, E. Rogers. ILC for FES-based Stroke Rehabilitation of Hand and Wrist. *IEEE Multi-Conference on System and Control*, 1267-1272, 2012.

[21] Y. Wang, E. Dassau, and F.J. Doyle III. Closed-loop control of artificial pancreatic beta-cell in Type 1 diabetes mellitus using model predictive iterative learning control. *IEEE Transactions on Biomedical Engineering*, 57(2):211-19, 2010.

[22] Y. Wang, F. Gao, and F.J. Doyle III. Survey on iterative learning control, repetitive control, and run-to-run control. *Journal of Process Control*, 19:1589–1600, 2009.

[23] S. Weber, D. Strommenger, U. Kertzscher, K. Affeld. Continuous blood pressure measurement with ultrasound. *Biomedizinische Technik*, 57(1):407–410, 2012.

[24] S. Weber, U. Kertzscher, K. Affeld. Measuring Blood Pressure using Ultrasound-Doppler Signals. (article in German), *Biomedizinische Technik*, 55:29-32, 2010.